Chemosphere 238 (2020) 124607

Contents lists available at ScienceDirect

Chemosphere

journal homepage: www.elsevier.com/locate/chemosphere

Fluoride-induced renal dysfunction via respiratory chain complex abnormal expression and fusion elevation in mice

Hong-wei Wang*, Shi-quan Zhu, Jing Liu, Cheng-yi Miao, Yan Zhang, Bian-hua Zhou**

College of Animal Science and Technology, Henan University of Science and Technology, Luoyang, 471000, Henan, People's Republic of China

HIGHLIGHTS

- Fluoride induced renal function disorder.
- Fluoride induced kidney structure damage.
- Fluoride inhibited renal cells proliferation.
- Fluoride interfere the expression of mitochondrial respiratory chain complexes.
- Fluoride elevates mitochondrial fusion.

ARTICLE INFO

Article history:
Received 10 July 2019
Received in revised form
15 August 2019
Accepted 16 August 2019
Available online 17 August 2019

Handling Editor: A. Gies

Keywords:
Fluoride
Kidney
Respiratory chain complexes
Mitochondrial fusion

ABSTRACT

A fluoride exposure mouse model is established to evaluate the relationship between mitochondrial respiratory chain complexes and renal dysfunction. Morphological changes in kidney tissues were observed. Renal function and cell proliferation in the kidneys were evaluated. The expression of mitochondrial fusion protein including mitofusin-1 (Mfn1) and optic atrophy 1 (OPA1), and mitochondrial respiratory chain complex subunits, including NDUFV2, SDHA, CYC1 and COX Ⅳ, were detected via real-time polymerase chain reaction, immunohistochemistry staining and Western blot, respectively. Results showed that the structures of renal tubule, renal glomerulus and renal papilla were seriously damaged. Renal function was impaired, and cell proliferation was remarkably inhibited by excessive fluoride in kidney. The mRNA and protein expression levels of Mfn1, OPA1, NDUFV2, CYC1 and COX Ⅳ were significantly increased after excessive fluoride exposure. However, the mRNA and protein expression of SDHA significantly decreased. Overall, our findings revealed that excessive fluoride can damage kidney structure, inhibit renal cell proliferation, interfere with the expression of mitochondrial respiratory chain complexes and elevate mitochondrial fusion. Consequently, renal function disorder occurred.

1. Introduction

Kidney is a highly metabolically active organ that plays an important role in removing metabolites from the plasma and in maintaining the homeostasis of water, electrolytes and pH. Oxidative phosphorylation of mitochondria is vital in ATP production to sustain the reabsorption and secretion function of renal tubule cells (Hall et al., 2009). Kidney function is highly related to the energy production of the mitochondria, and mitochondrial dysfunction is associated with diabetic and chronic kidney disease (Forbes and Thorburn, 2018; Galvan et al., 2017; Che et al., 2014). Mitochondrial fusion is essential for complementation of damaged mitochondrial DNAs and the maintenance of membrane potential for the physiological functions of the mitochondria (Cao et al., 2017; Franco et al., 2016). Mitofusin-1 (Mfn1) and optic atrophy 1 (OPA1) are dynamin proteins possess membrane-remodelling properties. Mfn1 and OPA1 mediate the fusion of outer and inner membranes of the mitochondria, respectively (Friedman and Nunnari, 2014; Lee and Yoon, 2016). However, an abnormal OPA1 expression leads to the fragmentation of the mitochondrial network, resulting in the permeabilisation of the outer mitochondrial membrane (Liesa et al., 2009; Elgass et al., 2013). The expression of decreased Mfn1 and

* Corresponding author. College of Animal Science and Technology, Henan University of Science and Technology, Kaiyuan Avenue 263, Luoyang, 471000, Henan, People's Republic of China.
** Corresponding author.
E-mail addresses: wanghw@haust.edu.cn (H.-w. Wang), zhusq@stu.haust.edu.cn (S.-q. Zhu), Liuj@stu.haust.edu.cn (J. Liu), miaocy@stu.haust.edu.cn (C.-y. Miao), zhangy@stu.haust.edu.cn (Y. Zhang), zhoubh@haust.edu.cn (B.-h. Zhou).

https://doi.org/10.1016/j.chemosphere.2019.124607
0045-6535/

increased fission-1(Fis1) may be involved in the increased oxidative stress in the kidney of chronic fluorosis rats (Qin et al., 2015). Some studies have also indicated that the mutation of OPA1 and Mfn genes is involved in neurodegenerative disease, such as dominant optic atrophy and Charcot-Marie-Tooth subtype 2A (Youle et al., 2012; Khacho and Slack, 2018). Therefore, the disruption of fusion causes mitochondrial dysfunction, further affecting kidney function.

Mitochondria respiratory chain is a redox and protonic coupling centre in oxidative phosphorylation and the main source of ATP production (Papa et al., 2012). Mitochondrial respiratory chain complexes, which are important components of the mitochondrial respiratory chain, are multi-subunit membrane protein complexes, including complexes I, II, III, IV. NDUFV2, SDHA, CYC1, COX IV, indispensable for assembly and function of the mitochondrial respiratory chain, are subunit of mitochondria complex I, II, III, IV. Mitochondrial complex I is responsible for NADH-catalysed oxidation by ubiquinone, and complex II can oxidation succinate into fumarate in the TCA cycle (Stroud et al., 2016; Korge et al., 2017). Complex I combines with complexes III and IV in the form of a supercomplex, which produces a transmembrane proton gradient for ATP synthesis (Lapuente-Brun et al., 2013). Complex IV, the terminal oxidase of the mitochondrial respiratory chain, can accept electrons from cytochrome *c* and transfer them to molecular oxygen to generate water (Little et al., 2018). Complex IV deficiencies cause subsequent loss of complex I, and the deficiency of mitochondrial complex I is associated with diverse cardiovascular diseases (Diaz et al., 2006; Forte et al., 2019). Complex I and complex III are generally considered the principal sites for ROS production (Chen et al., 2003b). Impaired mitochondrial respiratory chain complexes may result in ROS accumulation and decrease the synthesis of ATP involved in cell death (Baldissera et al., 2017). Thus, mitochondrial function is closely related to the normal expression of mitochondrial respiratory chain complexes.

Fluoride (F) has strong mitochondrial toxicity. Various studies have shown that excess F intake can induce mitochondria damage, leading to the release of Cyt *c* and the activation of caspase cascade, thereby causing apoptosis (Tan et al., 2018; Wang et al., 2017a, 2017b). Oxidative stress and lipid peroxidation are putative mechanisms of F toxicity. However, the underlying mechanisms of F-induced kidney dysfunction remain unclear. In this study, a mouse model of F-induced renal lesion was established to investigate the mechanism of F induced nephrotoxicity. The functions of the kidney and the mitochondrial respiratory chain were evaluated, and kidney cell proliferation was analysed through Bromodeoxyuridine (BrdU) measurement.

2. Materials and methods

2.1. Experimental animals

Forty-eight 30-day-old healthy Kunming mice were obtained from the Experimental Animal Centre of Zhengzhou University and kept in a standard animal house with air conditioning at 22−25 °C under hygienic conditions.

2.2. Establishment of the F-exposed mouse model

After a week of balanced feeding, the experimental mice were randomly divided into four groups of 12. The experiment was designed as follows: mice in the control group were given distilled water and fed with a standard diet; mice in the fluorine groups were given drinking water containing 25, 50 and 100 mg/L F^- and fed with a standard diet. On the 90th day of F exposure, the mice were anesthetised with 20% urethane (ethyl carbamate) solution. Blood was collected by cardiac puncture, and the serum was prepared. Serum samples were stored at −80 °C for preservation. The kidney was carefully removed and rapidly fixed in 10% formaldehyde for histopathological observation. This study design was approved by the Institutional Animal Care and Use Committee of China.

2.3. Histopathological observation

After the kidney tissues were fixed in 10% formaldehyde, the kidney tissue was dehydrated in different ethyl alcohol concentrations, rendered transparent in xylene, embedded in paraffin, continuously sliced to 5 μm and stained with haematoxylin and eosin. The sections were observed under a light microscope.

2.4. Assay of the renal function

The serum biochemical indices of calcium (Ca), phosphorus (P), creatinine (CREA), urea and uric acid (UA) were measured in accordance with the standard procedures by using an Automatic biochemical Analyzer (Rayto Life and Analytical Sciences Co., Ltd, Shenzhen, China).

2.5. BrdU measurement

BrdU measurement was conducted in accordance with the manufacturer's instructions (Servicebio, Wuhan, China). On the 90th day of fluorine treatment, the mice were intraperitoneally injected with BrdU. The experimental procedure was as follows: 0.3 mL of the BrdU solution (10 mg/mL) was intraperitoneally injected once every 2 h (four times in total). After the last injection of BrdU for 24 h, the mice were sacrificed, and their kidneys were carefully collected for immunohistochemistry (IHC) assay.

2.6. IHC staining

The paraffin tissue was serially sliced to 5 μm, dewaxed in xylene, rehydrated in different concentrations of ethyl alcohol and washed with distilled water. The sections were blocked with 5% bovine serum, incubated with specific Mfn1 (13798-1-AP, Proteintech Group Inc., Wuhan, China), OPA1 (27733-1-AP, Proteintech Group Inc., Wuhan, China), NDUFV2 (15301-1-AP, Proteintech Group Inc., Wuhan, China), SDHA (14865-1-AP, Proteintech Group Inc., Wuhan, China), CYC1 (10242-1-AP, Proteintech Group Inc., Wuhan, China), COX IV (10242-1-AP, Proteintech Group Inc., Wuhan, China) at 4 °C in a humidified chamber overnight and washed with phosphate buffered solution thrice. The sections were incubated with secondary antibody for 50 min at room temperature and stained with 3,3-diaminobenzidine. They were counterstained with haematoxylin and washed with tap water. IHC micrographs were observed under a microscope.

2.7. Quantitative real-time PCR

Total cellular RNA was extracted from the kidney tissue by using TRIzol reagent (Invitrogen, USA) and cDNA was further synthesised in accordance with the manufacturer's instruction. The specific primers for Mfn1, OPA1, NDUFV2, SDHA, CYC1 and COX IV were designed using Primer 5.0. Real-time PCR was performed using an Mx3000pTM real-time PCR system (Stratagene, USA) and a SYBR ® premix Ex Taq™ (Perfect Real Time) Kit (Takara, China). The relative expression levels of target genes were normalised to β-actin.

2.8. Western blot analysis

The kidney tissues were homogenised in lysis buffer and washed twice with ice-cold PBS. The homogenate was subsequently centrifuged at 12,000×*g* for 5 min at 4 °C. Afterwards, the supernatants were used to determine protein concentrations and normalised to a concentration equal to that of the protein. The supernatant protein was separated through SDS-PAGE and transferred onto polyvinylidene membrane. The membranes were blocked using 5% nonfat milk, and immunoblotting was performed by incubating the membranes with Mfn1, OPA1, NDUFV2, SDHA, CYC1, COX IV primary and secondary antibodies. Protein bands on the membranes were detected via enhanced chemiluminescence.

2.9. Statistical analysis

Experimental data were expressed as mean ± standard deviation. Statistical and data analyses were performed by *t*-test, and $P < 0.05$ was considered statistically significant.

3. Results

3.1. Effects of F on the histological structure of mouse kidney

As shown in Fig. 1, the cells of the renal glomerulus, the renal tubule and the renal papilla of the mice were neatly arranged with a normal histological structure in the control group. The shapes of the cells were regular and had a clear boundary (Fig. 1A1, A2 and A3). The kidney of the cells from F 25 group slightly changed (Fig. 1B1, B2 and B3). However, in the F 50 and 100 groups, the space of renal capsule was enlarged and the glomerulus was atrophied as the dose of F increased (Fig. 1C1 and D1). The cells of renal tubule and the renal papilla exposed to excessive fluoride were irregularly arranged, resulting in cell swelling, light-stained nuclei (Fig. 1C2, C3 and D3) and even cell breakage (Fig. 1D2).

3.2. BrdU measurement assay

The results of BrdU measurement in the kidney tissues are shown in Fig. 1. In the control group, BrdU-labelled kidney tissue exhibited a positive expression in the renal glomerulus, the renal tubule and the renal papilla (Fig. 1A4, A5 and A6). This finding indicated that cells remarkably proliferated in the kidney. In the F 25 group, the cells also exhibited a positive expression in the renal glomerulus, the renal tubule and the renal papilla (Fig. 1B4, B5 and B6). As the F dose intake increased, the positive expression of BrdU-labelled kidney tissue was remarkably down-regulated in the F 50 and 100 groups (Fig. 1C4, C5, C6, D4, D5 and D6). This result suggested that cell proliferation in renal glomerulus, the renal tubule and the renal papilla was inhibited. The relative densities of BrdU in the renal glomerulus, the renal tubule and the renal papilla were markedly down-regulated as the F intake increased (Fig. 1E, F and G).

3.3. Effects of F on renal function in mice

Renal function was measured by the changes in biomarkers (Ca, P, CREA, urea and UA) after fluoride exposure for 90 days. Table 1 shows that the serum concentrations of Ca and P were significantly decreased in the F 50 and 100 groups compared with that in the control group ($P < 0.05$). The serum concentration of CREA was significantly decreased in the F 100 group compared with that in the control group ($P < 0.05$). The serum concentration of UA was significantly increased in the sera of F 50 and 100 groups compared with that of the control group ($P < 0.01$), whereas the concentration of urea was not significantly changed.

3.4. Effects of fluoride on mitochondrial fusion in kidneys

The mRNA and protein expression levels of OPA1 and Mfn1 in the kidney are shown in Fig. 2. As presented in the IHC results, the expression levels of OPA1 and Mfn1 increased in F groups compared with that in the control group (Fig. 2A). Real-time PCR showed that the mRNA expression levels of Mfn1 and OPA1 significantly increased in the fluoride group ($P < 0.01$) (Fig. 2B). Western blot analysis revealed that the expression levels of Mfn1 and OPA1 were significantly up-regulated in this study ($P < 0.01$) (Fig. 2C and D).

3.5. Effects of fluoride on the expression of the subunits of mitochondrial respiratory chain complexes in the kidney

In Fig. 3, the mRNA and protein expression of NDUFV2 in the kidney was determined after F exposure. IHC showed that the expression of NDUFV2 increased in the fluoride group as the fluoride dose increased (Fig. 3A). Real-time PCR revealed that the mRNA expression of NDUFV2 significantly increased in the F 50 and 100 groups ($P < 0.01$) (Fig. 3B). Western blot analysis demonstrated that the expression level of NDUFV2 significantly increased in the F 50 and 100 groups ($P < 0.05$) (Fig. 3C and D).

Fig. 4 shows the mRNA and protein expression of SDHA in the kidney. As exhibited in the IHC results, the expression of SDHA decreased as F dose increased (Fig. 4A). Real-time PCR showed that the mRNA expression of SDHA significantly decreased in the F groups ($P < 0.01$) (Fig. 4B). Western blot analysis demonstrated that the expression level of SDHA was significantly down-regulated in the F 50 and 100 groups ($P < 0.05$) (Fig. 4C and D).

The mRNA and protein expression levels of CYC1 in the kidney are shown in Fig. 5. IHC showed that the expression of CYC1 was up-regulated as the F dose increased (Fig. 5A). Real-time PCR demonstrated that the mRNA expression of CYC1 significantly increased in the fluoride group ($P < 0.01$) (Fig. 5B). Western blot analysis revealed that the expression level of CYC1 significantly increased in the F 50 and 100 groups ($P < 0.05$) (Fig. 5C and D).

Fig. 6 presents the mRNA and protein expression levels of COX IV in the kidney. IHC result showed that the expression of COX IV increased as the F dose increased (Fig. 6A). Real-time PCR showed that the mRNA expression of COX IV significantly increased in the fluoride group ($P < 0.01$) (Fig. 6B). Western blot analysis demonstrated that the expression level of COX IV significantly increased in the F 50 and 100 groups ($P < 0.05$) (Fig. 6C and D).

4. Discussion

Kidney is a crucial organ in eliminating metabolites and toxic substances in vivo. It is vulnerable to invasion and damage by toxins or toxicants. The renal tubular epithelial cells, endothelial cells and sertoli cells are the constituent cells of the key point in renal tubules, renal glomeruli and renal papilla, respectively, which play crucial roles in the reabsorption, hemofiltration rate and excretion function of the kidneys (Antonio et al., 2017; Kido et al., 2017). Thus, these cells damage or proliferation inhibition will seriously affect kidney function. The cell proliferation is the basis of maintaining structure of organs, the proliferation of renal tubular epithelial cells, endothelial cells and sertoli cells in kidney was inhibited by F might be closely related to the structure damage of kidney. In this study, F could induce the damage of renal tubules, renal glomeruli and renal papilla in a dose-dependent way. Cell proliferation was remarkably inhibited by excessive F in the kidneys. F damages the structure of kidney and inhibits cell proliferation, further affecting

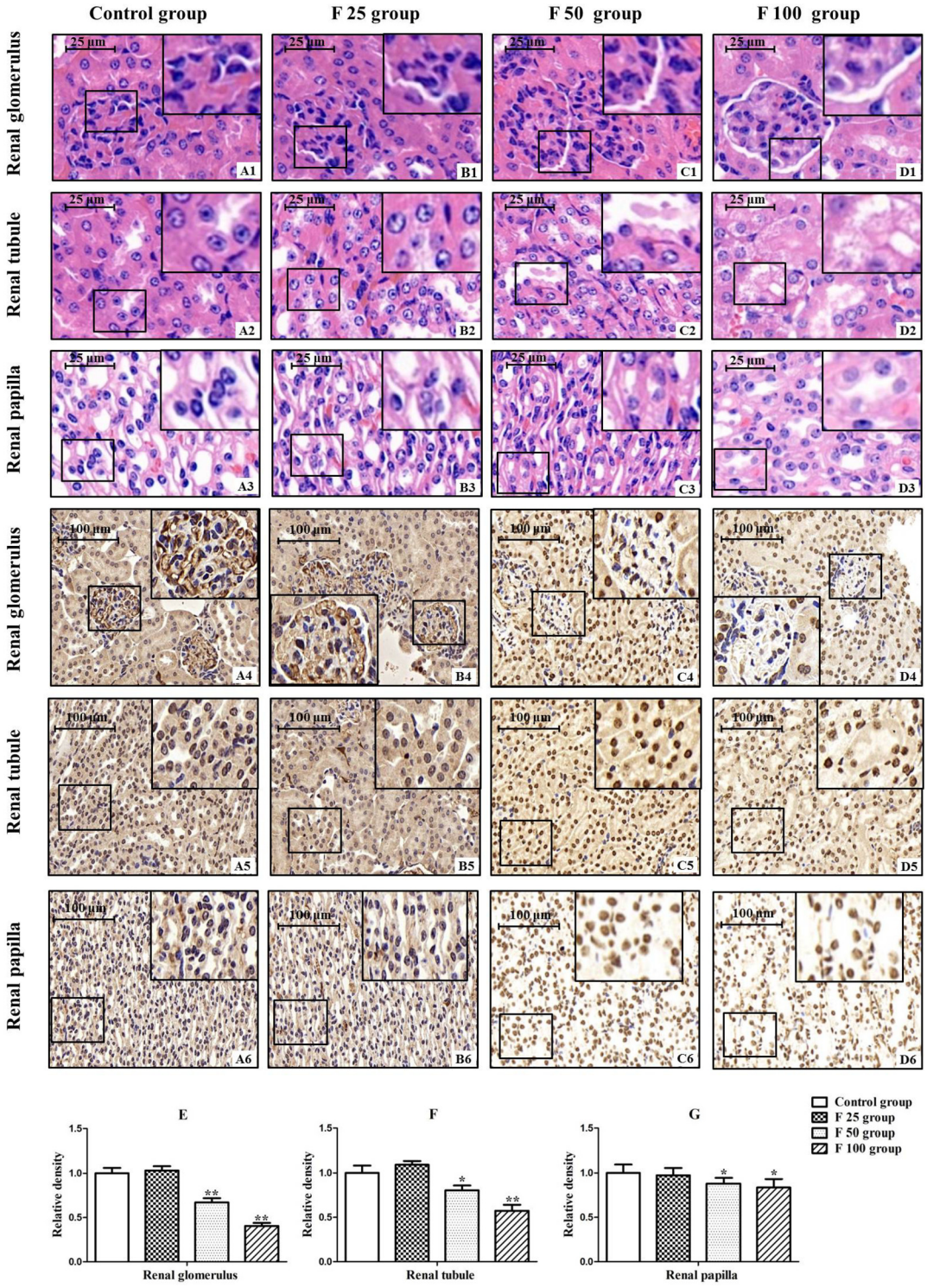

Fig. 1. Effect of fluoride on the histological morphology and cell proliferation in the kidney tissue. A1, A2 and A3 are the sections in the control group; B1, B2 and B3 are the sections in the F 25 group; C1, C2 and C3 are the sections of the kidney in the F 50 group; D1, D2 and D3 are the sections of the kidney in the F 100 group; A4, A5 and A6 are Brdu labelled kidney tissue in the control group; B4, B5 and B6 are Brdu labelled kidney tissue in the F 25 group; C4, C5 and C6 are Brdu labelled kidney tissue in the F 50 group; D4, D5 and D6 are Brdu labelled kidney tissue in the F 100 group. E, F and G are Relative densities of BrdU in the kidney tissues. $^{*}P < 0.05$ and $^{**}P < 0.01$ (the F group compared with the control group).

kidney functions and altering Ca and P metabolism. Ca and P play important roles in bone remodelling by bone resorption and bone formation, promoting bone formation and growth (Peacock, 2010). F can induce a decrease in Ca contents in faeces and blood and significantly increase the concentration of intracellular calcium, further leading to Ca^{2+} overload and endoplasmic reticulum stress in cells (Wang et al., 2018; Zhang et al., 2016b; Xu et al., 2007). Calcium ion is a crucial intracellular messenger in many signal transduction systems (Carafoli and Krebs, 2016). An abnormal Ca concentration results in cellular dysfunction. In this study, Ca and P

Table 1
Effect of F on kidney function (Ca, P, CREA, UA, UREA) in the serum of mice (Mean ± SD, n = 6).

Groups	Ca (mmol/L)	P (mmol/L)	CREA (μmol/L)	UA (μmol/L)	UREA (mmol/L)
Control group	2.46 ± 0.01	2.78 ± 0.17	68.12 ± 3.86	145.76 ± 6.58	9.03 ± 0.62
F 25 group	2.34 ± 0.08	2.75 ± 0.38	67.24 ± 5.67	152.54 ± 13.64	9.92 ± 0.68
F 50 group	2.28 ± 0.08**	2.23 ± 0.21**	64.96 ± 7.05	212.48 ± 30.97**	9.76 ± 0.85
F 100 group	2.28 ± 0.06**	2.35 ± 0.24*	60.86 ± 3.35*	253.96 ± 30.29**	9.07 ± 0.28

*$P < 0.05$ and **$P < 0.01$ (fluoride group compared with the control group).

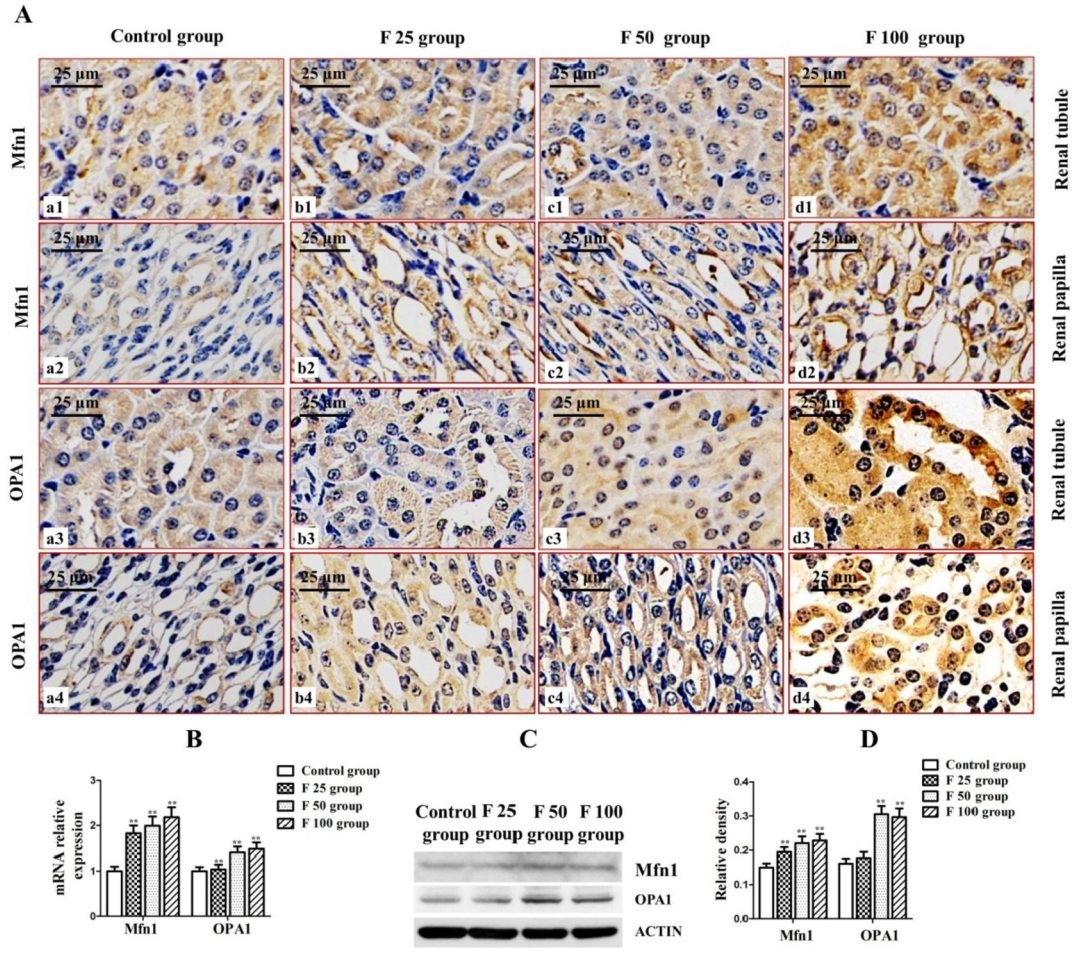

Fig. 2. Effects of fluoride on mitochondrial fusion protein expression in kidney tissue. (A) Immunohistochemistry of Mfn1 and OPA1 expressions in kidney tissue. (B) mRNA expression of Mfn1 and OPA1 in kidney detected by real-time PCR. (C) Western blot electrophoretic pattern. (D) Relative expression levels of Mfn1 and OPA1 in kidney tissue detected by Western blot. β-actin was used as a control. *$P < 0.05$ and **$P < 0.01$ (fluoride group compared with the control group).

concentrations significantly decreased, suggesting that F could affect renal function and disturb Ca and P metabolism.

CREA, UA and urea concentrations serve as biomarkers in serum to reflect renal function. CREA is a metabolic product of muscles in organisms and mainly excreted by filtration in the glomerulus. The concentration of CREA is implicated in the function of glomerular filtration and widely used to measure renal function (Levey et al., 1988; Myers et al., 2006). UA and urea levels associated with renal function are usually accompanied by kidney injury. UA is the final product of purine metabolism and exists largely as urate anion at physiological pH (Fathallah-Shaykh and Cramer, 2014). The reduced glomerular filtration rate leads to an increased serum UA, which is involved in hyperuricaemia (Giordano et al., 2015). The excessive accumulation of UA in serum is toxic to the body and implicated in gout, hypertension and cardiovascular diseases (Abeles, 2015). Urea is the ultimate product of protein metabolism and eliminated by the kidney. An abnormal urea concentration in serum can induce the apoptosis of vascular smooth muscle cells, promoting vascular calcification (Lau and Vaziri, 2017). F-induced nephrotoxicity is associated with kidney dysfunction. When renal function deteriorates, the elimination of F is also reduced, resulting in excessive F accumulation in kidneys and aggravating F toxicity (Kido et al., 2017). Therefore, normal kidney function plays a crucial role in reducing the accumulation of F in vivo. In this study, the serum levels of CREA and UA significantly increased; however, the urea concentration was not altered significantly. These results indicated that F could induce changes in renal biochemical indicators and cause kidney dysfunction.

Mitochondrion is a crucial target for various environmental pollutants. Our previous study showed that F can severely damage mitochondrial structure, leading to mitochondrial crista dissolution and vacuolisation (Tan et al., 2018; Zhou et al., 2018). Mitochondrial

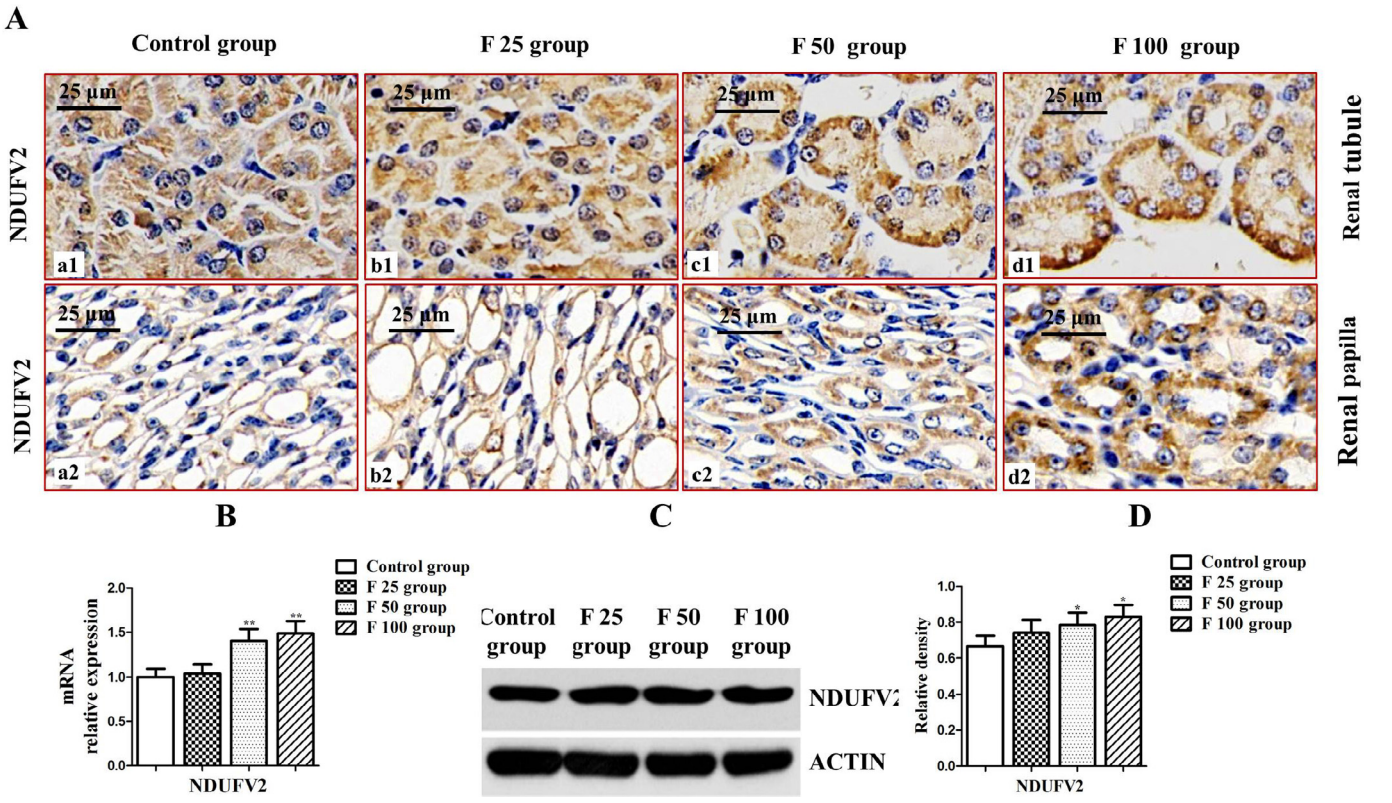

Fig. 3. Effects of fluoride on NDUFV2 expression in kidney tissue. (A) Immunohistochemistry of NDUFV2 expression in kidney tissue. (B) mRNA expression of NDUFV2 in kidney tissue detected by real-time PCR. (C) Western blot electrophoretic pattern. (D) Relative expression level of NDUFV2 in kidney tissue detected by Western blot. β-actin was used as a control. $^{*}P < 0.05$ and $^{**}P < 0.01$ (fluoride group compared with the control group).

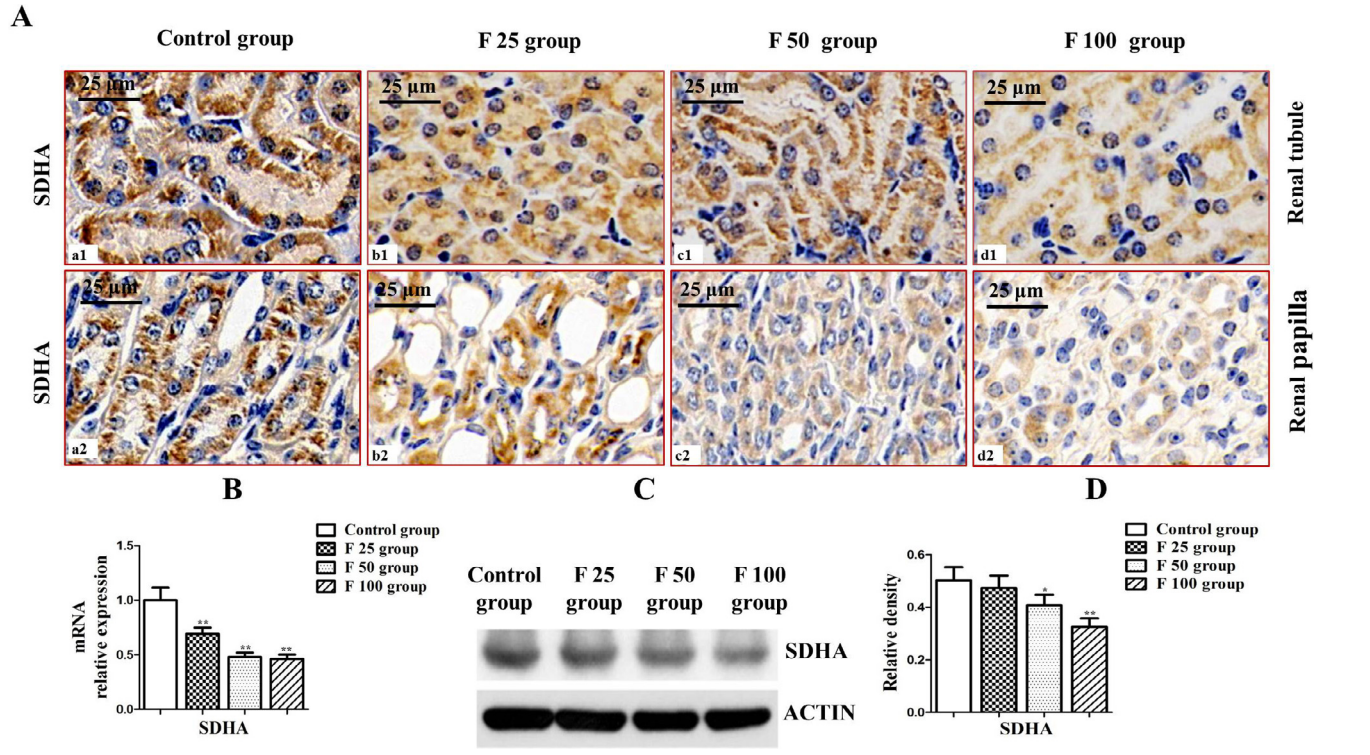

Fig. 4. Effects of fluoride on SDHA expression in kidney tissue. (A) Immunohistochemistry of SDHA expression in kidney tissue. (B) mRNA expression of SDHA in kidney tissue detected by real-time PCR. (C) Western blot electrophoretic pattern. (D) Relative expression level of SDHA in kidney tissue detected by Western blot. β-actin was used as a control. $^{*}P < 0.05$ and $^{**}P < 0.01$ (fluoride group compared with the control group).

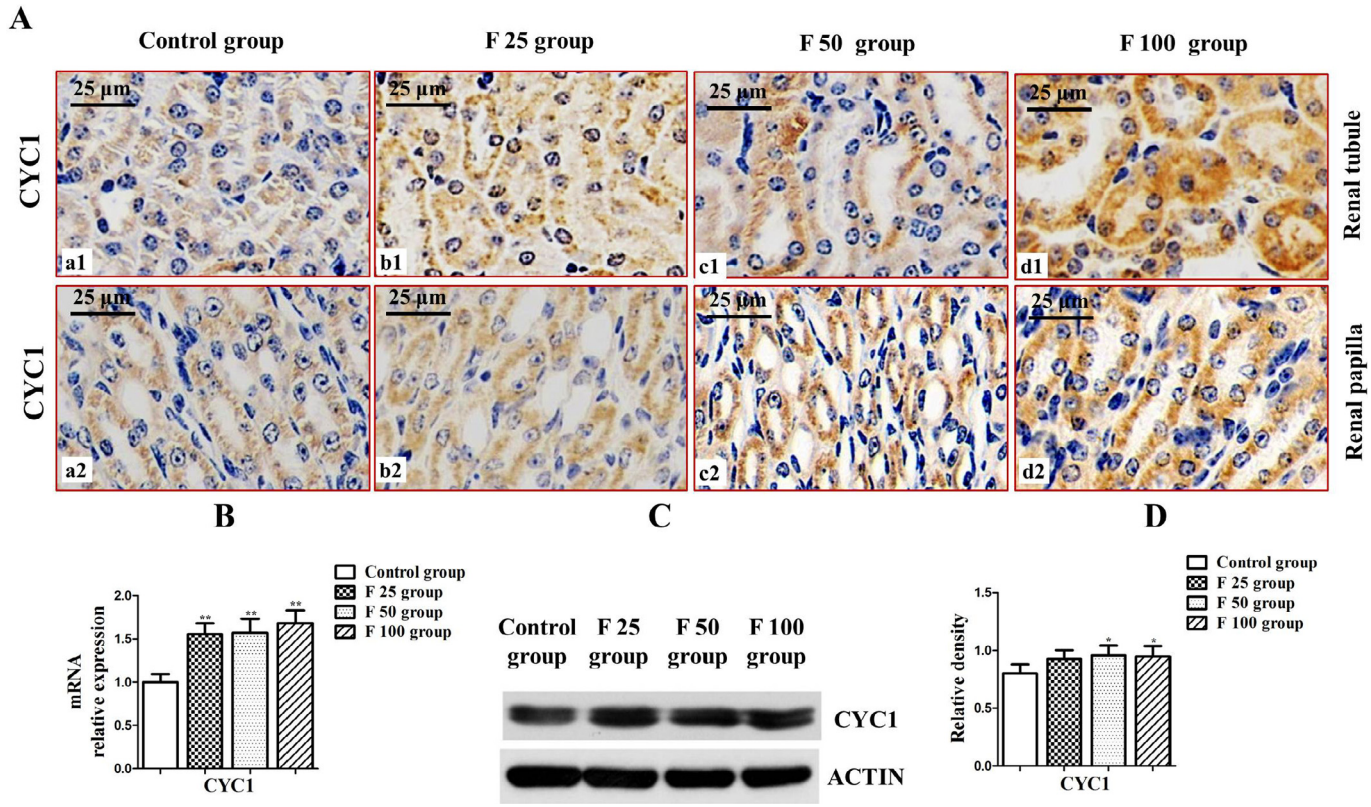

Fig. 5. Effects of fluoride on CYC1 expression in kidney tissue. (A) Immunohistochemistry of CYC1 expression in kidney tissue. (B) mRNA expression of CYC1 in kidney tissue detected by real-time PCR. (C) Western blot electrophoretic pattern. (D) Relative expression level of CYC1 in kidney tissue detected by Western blot. β-actin was used as a control. $^{*}P < 0.05$ and $^{**}P < 0.01$ (fluoride group compared with the control group).

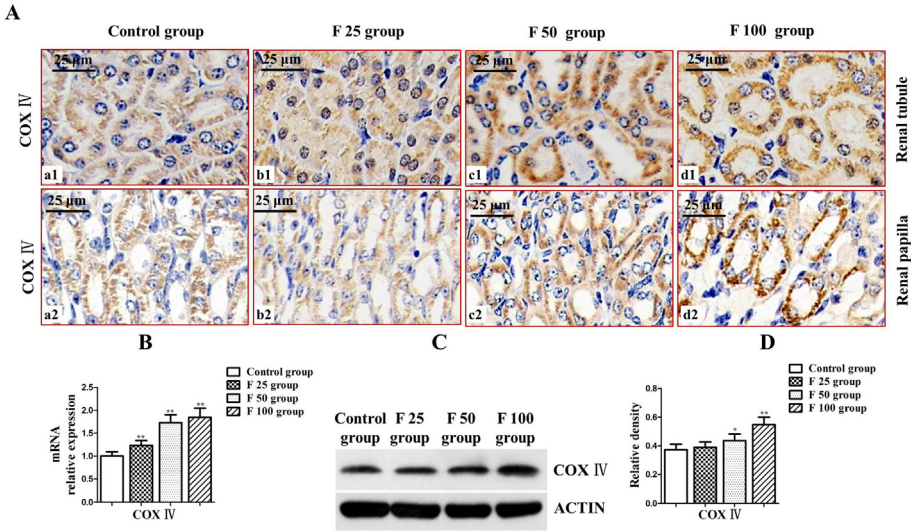

Fig. 6. Effects of fluoride on COX IV expression in kidney tissue. (A) Immunohistochemistry of COX IV expression in kidney tissue. (B) mRNA expression of COX IV in kidney tissue detected by real-time PCR. (C) Western blot electrophoretic pattern. (D) Relative expression level of COX IV in kidney tissue detected by Western blot. β-actin was used as a control. $^{*}P < 0.05$ and $^{**}P < 0.01$ (fluoride group compared with the control group).

respiratory chain complexes are located in mitochondrial cristae, and the breakup of mitochondrial crista seriously affects respiratory chain function. As one of the recognised mechanisms of F toxicity, F can induce mitochondrial damage by oxidative stress (Zhou et al., 2015; Wang et al., 2017b). The inhibition of the activities of mitochondrial respiratory chain complexes is related to ROS production, which is responsible for disease pathogenesis (Baldissera et al., 2017). Excessive ROS accumulation leads to mitochondrial damage that induces the opening of mPTP, the release of Cyt *c* into the cytosol and the activation of caspase cascade (Ameeramja et al., 2016; Tan et al., 2018). Oxidative phosphorylation is a major process in ATP production that can be

disturbed by mitochondrial respiratory chain damage. Our previous study confirmed that fluoride can induce the abnormal expression of mitochondrial respiratory chain complexes, leading to an increased ROS expression and a decreased ATP production in ovarian granulosa cells (Zhao et al., 2019). To investigate the link between renal function and mitochondrial respiratory capacity, we detected the expression of mitochondrial respiratory chain complexes. The expression of CYC1 and COX IV was notably inhibited after excessive fluoride exposure. However, the expression of NDUFV2 did not change significantly, whereas the expression of SDHA markedly increased. These results suggested that excessive F exposure interfered with the expression of mitochondrial respiratory chain complexes, leading to an abnormal expression in the mitochondria. The abnormal expression of complex subunits indicated respiratory chain damage, which may be involved in mitochondrial dysfunction.

Mitochondrial fusion participates in mitochondrial homeostasis, and abnormal fusion leads to mitochondrial dysfunction. The normal expression of mitochondrial fusion protein plays an important role in mitochondrial morphology. Mfn1 and Mfn2 can mediate the mitochondrial outer membrane fusion and are essential for growth and development (Chen et al., 2003a; Zhang et al., 2016a). OPA1, which mediates the fusion of mitochondrial inner membranes, also plays a key role in crista remodelling (Lee et al., 2017). Mitochondrial crista morphology modulates mitochondrial respiration and determines the assembly and stability of respiratory chain supercomplexes (Cogliati et al., 2013; Varanita et al., 2015). Moreover, mitochondrial respiratory chain efficiency can be improved by the increased OPA1 levels (Civiletto et al., 2015). The expression level of OPA1 was significantly up-regulated in this study. The increased expression of OPA1 might be a compensatory response to impaired mitochondrial respiratory chain. The increased expression levels of MFN1 and OPA1 indicate that excessive fluoride intake can induce an increase in mitochondrial fusion in kidneys.

The measuring the expression of the mitochondrial respiratory chain complex and fusion protein showed that F could disturb the expression levels of mitochondrial respiratory chain complexes and enhance mitochondrial fusion to counteract the F-induced negative effect on mitochondrial dysfunction. F-induced mitochondrial dysfunction might be the key point of the inhibition of cell proliferation in kidneys. Kidney dysfunction could also confirm that F-induced renal damage is closely related to mitochondrial dysfunction. These findings demonstrated that mitochondrial respiratory chain and fusion might be associated with mitochondrial dysfunction, which occurred in kidney damage after excessive F exposure.

In conclusion, excessive F could damage kidney structure, inhibit renal cell proliferation, interfere with the expression of mitochondrial respiratory chain complexes and elevate mitochondrial fusion. Consequently, renal function disorder occurred.

Conflicts of interest

The authors declare that there is no conflict of interest.

Acknowledgements

This work is sponsored by the National Natural Science Foundation of China (grant no. 31201963) and Young Backbone Teachers Training Project of Colleges and Universities in Henan Province, China (grant no. 2016GGJS-061).

References

Abeles, A.M., 2015. Hyperuricemia, gout, and cardiovascular disease: an update. Curr. Rheumatol. Rep. 17 (3), 13.
Ameeramja, J., Panneerselvam, L., Govindarajan, V., Jeyachandran, S., Baskaralingam, V., Perumal, E., 2016. Tamarind seed coat ameliorates fluoride induced cytotoxicity, oxidative stress, mitochondrial dysfunction and apoptosis in A549 cells. J. Hazard Mater. 301, 554–565.
Antonio, L.S., Jeggle, P., MacVinish, L.J., Bartram, J.C., Miller, H., Jarvis, G.E., Levy, F.M., Santesso, M.R., Leite, A.L., Oliveira, R.C., Buzalaf, M.A., Edwardson, J.M., 2017. The effect of fluoride on the structure, function, and proteome of a renal epithelial cell monolayer. Environ. Toxicol. 32 (4), 1455–1467.
Baldissera, M.D., Souza, C.F., Grings, M., Parmeggiani, B.S., Leipnitz, G., Moreira, K.L.S., da Rocha, M.I.U.M., da Veiga, M.L., Santos, R.C.V., Stefani, L.M., Baldisserotto, B., 2017. Inhibition of the mitochondrial respiratory chain in gills of Rhamdia quelen experimentally infected by Pseudomonas aeruginosa: Interplay with reactive oxygen species. Microb. Pathog. 107, 349–353.
Cao, Y.L., Meng, S., Chen, Y., Feng, J.X., Gu, D.D., Yu, B., Li, Y.J., Yang, J.Y., Liao, S., Chan, D.C., Gao, S., 2017. MFN1 structures reveal nucleotide-triggered dimerization critical for mitochondrial fusion. Nature 542 (7641), 372–376.
Carafoli, E., Krebs, J., 2016. Why calcium? How calcium became the best communicator. J. Biol. Chem. 291 (40), 20849–20857.
Che, R., Yuan, Y., Huang, S., Zhang, A., 2014. Mitochondrial dysfunction in the pathophysiology of renal diseases. Am. J. Physiol. Renal. Physiol. 306 (4), F367–F378.
Chen, H., Detmer, S.A., Ewald, A.J., Griffin, E.E., Fraser, S.E., Chan, D.C., 2003a. Mitofusins Mfn1 and Mfn2 coordinately regulate mitochondrial fusion and are essential for embryonic development. J. Cell Biol. 160 (2), 189–200.
Chen, Q., Vazquez, E.J., Moghaddas, S., Hoppel, C.L., Lesnefsky, E.J., 2003b. Production of reactive oxygen species by mitochondria: central role of complex III. J. Biol. Chem. 278 (38), 36027–36031.
Civiletto, G., Varanita, T., Cerutti, R., Gorletta, T., Barbaro, S., Marchet, S., Lamperti, C., Viscomi, C., Scorrano, L., Zeviani, M., 2015. Opa1 overexpression ameliorates the phenotype of two mitochondrial disease mouse models. Cell Metabol. 21 (6), 845–854.
Cogliati, S., Frezza, C., Soriano, M.E., Varanita, T., Quintana-Cabrera, R., Corrado, M., Cipolat, S., Costa, V., Casarin, A., Gomes, L.C., Perales-Clemente, E., Salviati, L., Fernandez-Silva, P., Enriquez, J.A., Scorrano, L., 2013. Mitochondrial cristae shape determines respiratory chain supercomplexes assembly and respiratory efficiency. Cell 155 (1), 160–171.
Diaz, F., Fukui, H., Garcia, S., Moraes, C.T., 2006. Cytochrome c oxidase is required for the assembly/stability of respiratory complex I in mouse fibroblasts. Mol. Cell. Biol. 26 (13), 4872–4881.
Elgass, K., Pakay, J., Ryan, M.T., Palmer, C.S., 2013. Recent advances into the understanding of mitochondrial fission. Biochim. Biophys. Acta 1833 (1), 150–161.
Fathallah-Shaykh, S.A., Cramer, M.T., 2014. Uric acid and the kidney. Pediatr. Nephrol. 29 (6), 999–1008.
Forbes, J.M., Thorburn, D.R., 2018. Mitochondrial dysfunction in diabetic kidney disease. Nat. Rev. Nephrol. 14 (5), 291–312.
Forte, M., Palmerio, S., Bianchi, F., Volpe, M., Rubattu, S., 2019. Mitochondrial complex I deficiency and cardiovascular diseases: current evidence and future directions. J. Mol. Med. 97 (5), 579–591.
Franco, A., Kitsis, R.N., Fleischer, J.A., Gavathiotis, E., Kornfeld, O.S., Gong, G., Biris, N., Benz, A., Qvit, N., Donnelly, S.K., Chen, Y., Mennerick, S., Hodgson, L., Mochly-Rosen, D., Dorn II., G.W., 2016. Correcting mitochondrial fusion by manipulating mitofusin conformations. Nature 540 (7631), 74–79.
Friedman, J.R., Nunnari, J., 2014. Mitochondrial form and function. Nature 505 (7483), 335–343.
Galvan, D.L., Green, N.H., Danesh, F.R., 2017. The hallmarks of mitochondrial dysfunction in chronic kidney disease. Kidney Int. 92 (5), 1051–1057.
Giordano, C., Karasik, O., King-Morris, K., Asmar, A., 2015. Uric acid as a marker of kidney disease: Review of the current literature. Dis. Markers 2015, 382918.
Hall, A.M., Unwin, R.J., Parker, N., Duchen, M.R., 2009. Multiphoton imaging reveals differences in mitochondrial function between nephron segments. J. Am. Soc. Nephrol. 20 (6), 1293–1302.
Khacho, M., Slack, R.S., 2018. Mitochondrial dynamics in the regulation of neurogenesis: from development to the adult brain. Dev. Dynam. 247 (1), 47–53.
Kido, T., Tsunoda, M., Sugaya, C., Hano, H., Yanagisawa, H., 2017. Fluoride potentiates tubulointerstitial nephropathy caused by unilateral ureteral obstruction. Toxicology 392, 106–118.
Korge, P., John, S.A., Calmettes, G., Weiss, J.N., 2017. Reactive oxygen species production induced by pore opening in cardiac mitochondria: the role of complex II. J. Biol. Chem. 292 (24), 9896–9905.
Lapuente-Brun, E., Moreno-Loshuertos, R., Acín-Pérez, R., Latorre-Pellicer, A., Colás, C., Balsa, E., Perales-Clemente, E., Quirós, P.M., Calvo, E., Rodríguez-Hernández, M.A., Navas, P., Cruz, R., Carracedo, Á., López-Otín, C., Pérez-Martos, A., Fernández-Silva, P., Fernández-Vizarra, E., Enríquez, J.A., 2013. Supercomplex assembly determines electron flux in the mitochondrial electron transport chain. Science 340 (6140), 1567–1570.
Lau, W.L., Vaziri, N.D., 2017. Urea, a true uremic toxin: the empire strikes back. Clin. Sci. 131 (1), 3–12.
Lee, H., Smith, S.B., Yoon, Y., 2017. The short variant of the mitochondrial dynamin OPA1 maintains mitochondrial energetics and cristae structure. J. Biol. Chem. 292 (17), 7115–7130.

Lee, H., Yoon, Y., 2016. Mitochondrial fission and fusion. Biochem. Soc. Trans. 44 (6), 1725–1735.
Levey, A.S., Perrone, R.D., Madias, N.E., 1988. Serum creatinine and renal function. Annu. Rev. Med. 39, 465–490.
Liesa, M., Palacín, M., Zorzano, A., 2009. Mitochondrial dynamics in mammalian health and disease. Physiol. Rev. 89 (3), 799–845.
Little, A.G., Lau, G., Mathers, K.E., Leary, S.C., Moyes, C.D., 2018. Comparative biochemistry of cytochrome c oxidase in animals. Comp. Biochem. Physiol. B Biochem. Mol. Biol. 224, 170–184.
Myers, G.L., Miller, W.G., Coresh, J., Fleming, J., Greenberg, N., Greene, T., Hostetter, T., Levey, A.S., Panteghini, M., Welch, M., Eckfeldt, J.H., 2006. Recommendations for improving serum creatinine measurement: a report from the laboratory working group of the National kidney disease education program. National Kidney Disease Education Program Laboratory Working Group Clin. Chem. 52 (1), 5–18.
Papa, S., Martino, P.L., Capitanio, G., Gaballo, A., De Rasmo, D., Signorile, A., Petruzzella, V., 2012. The oxidative phosphorylation system in mammalian mitochondria. Adv. Exp. Med. Biol. 942, 30–37.
Peacock, M., 2010. Calcium metabolism in health and disease. Clin. J. Am. Soc. Nephrol. 5 (Suppl. 1), S23–S30.
Qin, S.L., Deng, J., Lou, D.D., Yu, W.F., Pei, J., Guan, Z.Z., 2015. The decreased expression of mitofusin-1 and increased fission-1 together with alterations in mitochondrial morphology in the kidney of rats with chronic fluorosis may involve elevated oxidative stress. J. Trace Elem. Med. Biol. 29, 263–268.
Stroud, D.A., Surgenor, E.E., Formosa, L.E., Reljic, B., Frazier, A.E., Dibley, M.G., Osellame, L.D., Stait, T., Beilharz, T.H., Thorburn, D.R., Salim, A., Ryan, M.T., 2016. Accessory subunits are integral for assembly and function of human mitochondrial complex I. Nature 538 (7623), 123–126.
Tan, P.P., Zhou, B.H., Zhao, W.P., Jia, L.S., Liu, J., Wang, H.W., 2018. Mitochondria-mediated pathway regulates C2C12 cell apoptosis induced by fluoride. Biol. Trace Elem. Res. 185 (2), 440–447.
Varanita, T., Soriano, M.E., Romanello, V., Zaglia, T., Quintana-Cabrera, R., Semenzato, M., Menabò, R., Costa, V., Civiletto, G., Pesce, P., Viscomi, C., Zeviani, M., Di Lisa, F., Mongillo, M., Sandri, M., Scorrano, L., 2015. The OPA1-dependent mitochondrial cristae remodeling pathway controls atrophic, apoptotic, and ischemic tissue damage. Cell Metabol. 21 (6), 834–844.
Wang, H.W., Liu, J., Zhao, J., Lin, L., Zhao, W.P., Tan, P.P., Tian, W.S., Zhou, B.H., 2018. Ca^{2+} metabolic disorder and abnormal expression of cardiac troponin involved in fluoride-induced cardiomyocyte damage. Chemosphere 201, 564–570.
Wang, H.W., Zhao, W.P., Liu, J., Tan, P.P., Tian, W.S., Zhou, B.H., 2017a. ATP5J and ATP5H proactive expression correlates with cardiomyocyte mitochondrial dysfunction induced by fluoride. Biol. Trace Elem. Res. 180 (1), 63–69.
Wang, H.W., Zhao, W.P., Liu, J., Tan, P.P., Zhang, C., Zhou, B.H., 2017b. Fluoride-induced oxidative stress and apoptosis are involved in the reducing of oocytes development potential in mice. Chemosphere 186, 911–918.
Xu, H., Zhou, Y.L., Zhang, J.M., Liu, H., Jing, L., Li, G.S., 2007. Effects of fluoride on the intracellular free Ca2+ and Ca2+-ATPase of kidney. Biol. Trace Elem. Res. 116 (3), 279–288.
Youle, R.J., van der, Bliek, A.M., 2012. Mitochondrial fission, fusion, and stress. Science 337 (6098), 1062–1065.
Zhang, C., Shi, Z., Zhang, L., Zhou, Z., Zheng, X., Liu, G., Bu, G., Fraser, P.E., Xu, H., Zhang, Y.W., 2016a. Appoptosin interacts with mitochondrial outer-membrane fusion proteins and regulates mitochondrial morphology. J. Cell Sci. 129 (5), 994–1002.
Zhang, Y., Zhang, K., Ma, L., Gu, H., Li, J., Lei, S., 2016b. Fluoride induced endoplasmic reticulum stress and calcium overload in ameloblasts. Arch. Oral Biol. 69, 95–101.
Zhao, W.P., Wang, H.W., Liu, J., Zhang, Z.H., Zhu, S.Q., Zhou, B.H., 2019. Mitochondrial respiratory chain complex abnormal expressions and fusion disorder are involved in fluoride-induced mitochondrial dysfunction in ovarian granulosa cells. Chemosphere 215, 619–625.
Zhou, B.H., Tan, P.P., Jia, L.S., Zhao, W.P., Wang, J.C., Wang, H.W., 2018. PI3K/AKT signaling pathway involvement in fluoride-induced apoptosis in C2C12 cells. Chemosphere 199, 297–302.
Zhou, B.H., Zhao, J., Liu, J., Zhang, J.L., Li, J., Wang, H.W., 2015. Fluoride-induced oxidative stress is involved in the morphological damage and dysfunction of liver in female mice. Chemosphere 139, 504–511.